Survey of water vapor sources in the southern hemisphere

P. Kaufmann, S. Zisk,[a] E. Scalise Jr., R. E. Schaal, and R. H. Gammon[b]

Centro de Rádio Astronomia e Astrofísica, Universidade Mackenzie, São Paulo, Brasil

(Received 17 March 1977; revised 19 May 1977)

An extensive, low-flux-limit survey of southern hemisphere celestial water vapor sources has been carried out at Itapetinga Radio Observatory, Atibaia, Brazil. Observations were made at 115 different potential source positions, with upper limits for line detection ranging from 7 to 80 Jy. Fifteen new Galactic H_2O masers were discovered, and one weak one was confirmed. Some of them were found in H II regions in which type-I OH emission has not yet been detected. A selection of H II regions observed in the Carina Nebula yielded negative results. A survey of H II regions in the Magellanic Clouds also yielded negative results for the presence of very strong H_2O emitters.

INTRODUCTION

During 4–8 November 1975 and 18–21 May 1976, an intense observing program was carried out to look for new water vapor celestial masers in the southern hemisphere. (These two observing sessions are hereafter referred to as Run I and Run II, respectively.) For the detection of the $6_{16} \rightarrow 5_{23}$ rotational transition line of the water vapor molecule at 22.23508 GHz, a low-noise maser amplifier was built at Haystack Observatory, and installed on the 13.7-m Itapetinga radio telescope (Kaufmann *et al.* 1976).

There have been a number of previous searches for H_2O sources in the southern hemisphere with lower-limit line fluxes greater than or equal to 200 Jy (1 Jy = 10^{-26} W m^{-2} Hz^{-1}) (Johnston *et al.* 1971; Johnston *et al.* 1972; Caswell *et al.* 1974; Kaufmann *et al.* 1974a). A search for selected wide-spectrum H_2O sources has also been reported recently (Goss *et al.* 1975).

The present program was directed to lowering the existing detection limits. The limit actually achieved for line detection ranged from 7 to 80 Jy, depending on the integration time and the condition of the sky and the system.

Regarding the problem of flux calibration, there were some earlier gross discrepancies reported between measurements of absolute flux obtained at Parkes (Australia) and Itapetinga observatories (Kaufmann *et al.* 1974b). These discrepancies appear to have been resolved during the intervening period. Strong H_2O sources observed in June 1975 at Parkes (Goss *et al.* 1975) and at Itapetinga, within one week of each other, show the same absolute flux densities within a factor of 1.3. This minor difference is explainable as a result of the possible source variability and the difference in spectral resolution of the two radiometers.

The present survey was about 90% complete on known southern compact H II regions with type-I OH emitters. Preliminary results based on Run I have been reported elsewhere (Kaufmann *et al.* 1976). The present study also covered the most promising positions in Carina Nebula, and H II regions in the Large Magellanic Cloud. Observations were also carried on a selection of H II regions in the Small Magellanic Cloud.

[a] Visiting Scientist; permanent address: NEROC–Haystack Observatory, Westford, Massachusetts 01886.

[b] Now at Battelle, Seattle Research Center, Seattle, Washington.

I. EXPERIMENT

A new *K*-band ruby maser was constructed at Haystack Observatory for long-term loan to Itapetinga Observatory. It is a replica of the latest Haystack maser, which is based on the original design by Yngvesson *et al.* (1975).

The gain of the Itapetinga maser is about 25 dB at the H_2O transition frequency, when operated at a bath temperature of about 1.5 K. The excess receiver noise temperature is 30–50 K referred to the room-temperature input flange of the maser. Operation at frequencies from at least 22 to 25 GHz should be possible, but were not attempted in this series of experiments.

At Itapetinga Radio Observatory a new *K*-band mixer receiver was developed to follow the maser amplifier. When used as an independent receiver, its single sideband noise temperature is 600 K. The backend consists of a 47-channel spectrograph with 100-kHz filters, followed by a digital data-acquisition system. The apparent SSB system temperature of the complete maser receiver ranged from 200 to 350 K during the observations, based on output signal/noise ratio. This figure includes the sky emission contribution of 50–150 K, depending on the season (Marques dos Santos 1974; Fogarty 1975); the radome emission temperature of less than 10 K (Kaufmann *et al.* 1976); input waveguide and switch losses of about 100 K; and, in Run I, an unexplained excess-noise contribution, probably from short-term receiver gain fluctuations.

The 13.7-m Itapetinga telescope characteristics at *K* band have been described elsewhere (Kaufmann *et al.* 1976). Aperture efficiency was remeasured for this experiment during Run I, using Virgo A (assuming a flux

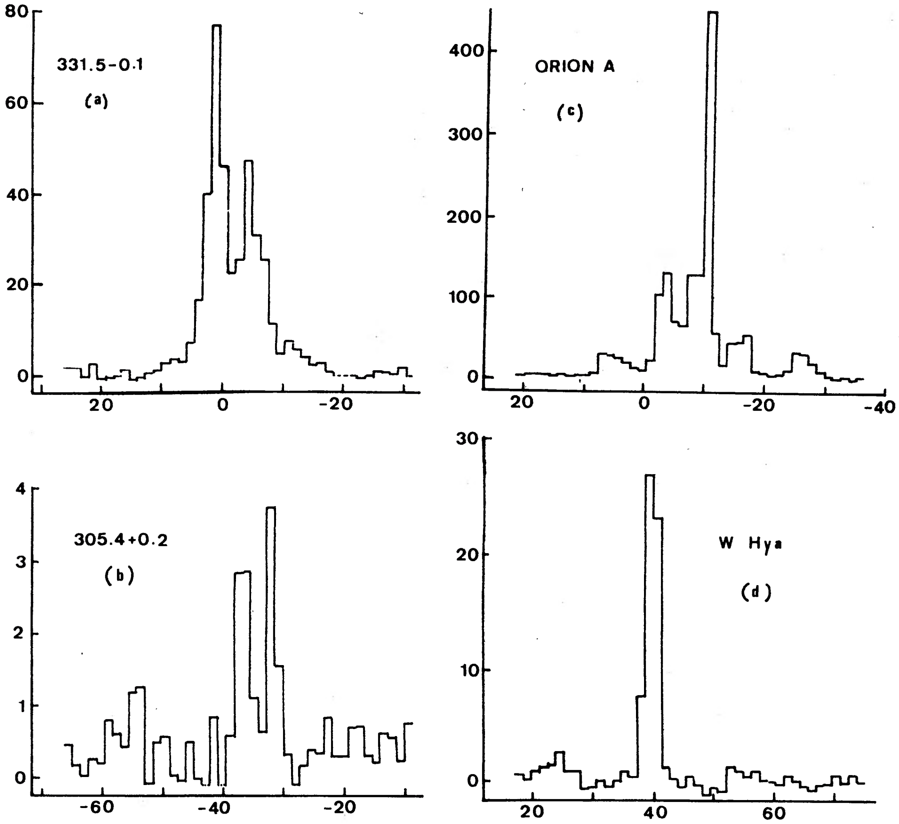

FIG. 1. Spectra of reference/calibration sources: (a) 331.5 − 0.1, (b) 305.4 + 0.2, (c) Orion A, (d) W Hydra. Abcissae are in km sec^{-1}, and ordinates in corrected antenna temperature (K).

of 21.4 Jy; Klein 1974) and Venus (assuming 420-K brightness temperature; Law and Staelin 1968) as calibrators. The resulting aperture efficiency was 54% at 50-deg elevation, in agreement with previous measurements (flux factor of 34.5 Jy/K). There is a small dependence of antenna gain on elevation which was included in the data reduction.

During Run I, sky conditions were quite poor for observing at water vapor frequencies. During Run II, the sky conditions were generally good, but several of the measurements were made during rain. The optical depth τ was determined frequently during this program from sky emission measurements (Fogarty 1975), and ranged from 0.2 to 0.5. Corrected antenna temperatures were obtained from the equation

$$T_a \text{ (corrected)} = T_a \text{ (observed) } (a/\eta_r) \exp(\tau \sec z),$$

where $\eta_r = 0.77$ is the radome transmission at 22.2 GHz, z is the zenith angle, and a is the antenna gain factor, varying from 1 at $z = 0°$ to 1.2 at $z = 60°$. Observed temperatures were referred to a calibrated gas-discharge noise tube. The reported flux densities refer to 100-kHz filter bandpass.

The feed consists of two rectangular horns, vertically polarized, placed near the Cassegrain focus. These produce two 4.5-arcmin-diameter beams, separated horizontally by 9.5 arcmin. The absolute pointing and tracking accuracy of the Itapetinga telescope is better than 0.25 arcmin, which is negligible compared to the beamwidth. Measurements were made with on–on beam switching; the antenna position was shifted every minute and the signals integrated for 48 sec. The typical run duration was 6 min (i.e., 4.8 min of integration time) during Run I, with interchannel peak-to-peak output fluctuation of about 40 Jy. During Run II the receiver was in better condition; the typical run duration was 10 min (i.e., 8-min integration), with peak-to-peak fluctuations of 18 Jy. For a number of observations, more than one run or longer runs were made; the corresponding upper detection limits are indicated in the Tables II–IV. For each observation a spectral range of at least ±28 km sec^{-1} was searched.

For test purposes we observed several known continuum and strong H_2O line sources in the southern sky during Run I. H_2O 331.5 − 0.1, our basic reference source, is shown in Fig. 1(a). The strong line at −96 km sec^{-1} has decreased in intensity since May 1975 (Goss *et al.* 1975). H_2O 305.4 + 0.2 is shown in Fig. 1(b). Two strong lines appear at about 32 and 37 km sec^{-1}, as reported by Johnston *et al.* (1972), but there is no longer a line at −40 km sec^{-1} as reported by Caswell *et al.* (1974). It is possible that this source is strongly variable or, alternatively, that the earlier spectrum was confused with 305.3 + 0.2, although the space separation of the two sources seems somewhat large [Table I(b)]. Orion

TABLE I. New H_2O Galactic sources discovered.

Source	Observed positions (1950.0) R.A.	Dec.	Center of radial velocity searched (km sec^{-1})	Comments
		(a) H_2O sources associated to type-I OH emitters		
309.9 + 0.5	$13^{h}47^{m}12^{s}.5$	$-61°19'58''$	-60	Fig. 2(a)
316.8 + 0.1	14 41 32.0	-59 36 54	-50	Fig. 2(b)
330.9 − 0.4	16 06 29.8	-51 57 38	-60	Fig. 2(c)
333.2 − 0.1	16 16 07.3	-50 07 48	-90	Fig. 2(d)
338.9 + 0.6	16 36 56.4	-45 35 53	-75	Fig. 2(e)
345.5 + 0.3	17 00 56.9	-40 39 38	-20	Fig. 2(f)
347.6 + 0.2	17 08 22.7	-39 05 09	-100	Fig. 2(g)
349.1 + 0.1	17 13 00.9	-37 56 06	$-80, -20$	Fig.2(h), confirmed
0.55 − 0.85	17 47 08.0	-28 53 06	$+13$	Fig. 2(i)
		(b) H_2O sources at H II regions for which OH main line emission is not known		
267.9 − 1.1	$08^{h}57^{m}23^{s}.0$	$-47°19'24''$	$+2$	Fig. 3(a)
284.3 − 0.3	10 22 20.0	-57 32 00	0	Fig. 3(b)
291.3 − 0.7	11 09 46.0	-61 02 36	-22	Fig. 3(c)
305.3 + 0.2	13 08 23.0	-62 17 30	-40	Fig. 3(d)
326.7 + 0.6	15 40 56.0	-53 57 24	$+5.2, -46, -97.2$	Fig. 3(e)
332.7 − 0.6	16 15 58.0	-50 56 00	-50	Fig. 3(f)
348.7 − 1.0	17 16 39.0	-38 54 36	-10	Fig. 3(g)

A H_2O is shown in Fig. 1(c); this source was used as a pointing calibrator. The long-period variable star W Hya [Fig. 1(d)] was intended as a calibrator because of its predictable variability (Schwartz *et al.* 1974). However, the observed intensity of its main line at 39 km sec^{-1} in November 1975 was 4 times larger than that predicted. It is possible that the radio variability of W Hya might be peculiar, perhaps because of its classification as a semiregular variable star (Kukarkin *et al.* 1969). Lépine (1977) has, indeed, suggested that the peak-to-peak intensity change of W Hya can vary by a factor of 10 from cycle to cycle. One maximum was observed in 1975, and a much smaller one in 1976.

II. NEW GALACTIC H_2O SOURCES ASSOCIATED WITH H II REGIONS

A. Type-I OH Sources

It is known that type-I OH Galactic sources which show emission at the main lines of 1665 and 1667 MHz often show H_2O maser emission at the same radial velocities (Turner and Rubin 1971). New discoveries of such emitters would depend largely on the sensitivity of the receiving system. We observed 24 type-I OH sources at their reported positions and radial velocities (Robinson *et al.* 1974; Caswell and Haynes 1975). Table I lists the eight newly discovered sources and the one confirmation (Turner and Rubin 1971), and Fig. 2 shows the corresponding spectra. No attempt was made to determine actual H_2O source positions.

H_2O 316.8 + 0.1 [Fig. 2(b)]. A strong water vapor source was seen in both Runs I and II. The figure shows the spectrum from Run I, with a 290-Jy line at -48.6 km sec^{-1}. Haynes *et al.* (1976) recently observed weak OH emission associated with this source.

H_2O 330.9 − 0.4 [Fig. 2(c)]. Examined by Caswell *et al.* (1974) to a flux limit of 190 Jy. The figure shows a weak source with a major line at -62.7 km sec^{-1} (45 Jy), observed during Run I.

H_2O 333.2 − 0.1 [Fig. 2(d)]. A newly discovered type-I OH source (Caswell and Haynes 1975), situated at one of the Galactic H II regions defined on the Goss and Shaver (1970) 5-GHz continuum maps. H_2O emission was found in Run I as a 59-Jy line at -84.6 km sec^{-1}.

H_2O 338.9 + 0.6 [Fig. 2(e)]. No H_2O emission was seen by Caswell *et al.* (1974) to a flux limit of 125 Jy. At the present epoch, a 127-Jy line was observed at -76.3 km sec^{-1} in Run I.

H_2O 345.5 + 0.3 [Fig. 2(f)]. The strongest source found in this class. Not detected by Caswell *et al.* (1974) to a limit of 115 Jy, but during Run I a strong 359-Jy line was seen at -28.1 km sec^{-1} and a weaker one (67 Jy) at -39.6 km sec^{-1}. In Run II, the strong line was confirmed, but the weaker feature had disappeared.

H_2O 347.6 + 0.2 [Fig. 2(g)]. This is a weak source, with intensity below the detection limit of the Caswell *et al.* (1974) source. The figure, from Run I, shows a 49-Jy line at -83.8 km sec^{-1} and a possible weaker line at -94.6 km sec^{-1}. In Run II only the -83.8 km sec^{-1} feature was confirmed, with a flux of 20 Jy.

H_2O 349.1 + 0.1 [Fig. 2(h)]. Not detected in the Johnston *et al.* (1972) survey. Turner and Rubin (1971) suggested a weak line at -78.3 km sec^{-1} (20 Jy). During Run II we observed two lines at -88.1 km sec^{-1} (53 Jy) and -80.0 km sec^{-1} (34 Jy), and a weaker line at -9.2 km sec^{-1} (16 Jy).

H_2O 0.55 − 0.85 [Fig. 2(i)]. Situated in a dense molecular cloud, this source is also known as RCW 142. OH, H_2CO, and H110α lines were observed by Gardner and Whiteoak (1975). The velocity of the major H_2O line at +13 km sec^{-1} (127 Jy) is in the vicinity of several OH emission lines. Another 30-km sec^{-1} H_2O line is present, but the -5.9-km sec^{-1} feature may be an arti-

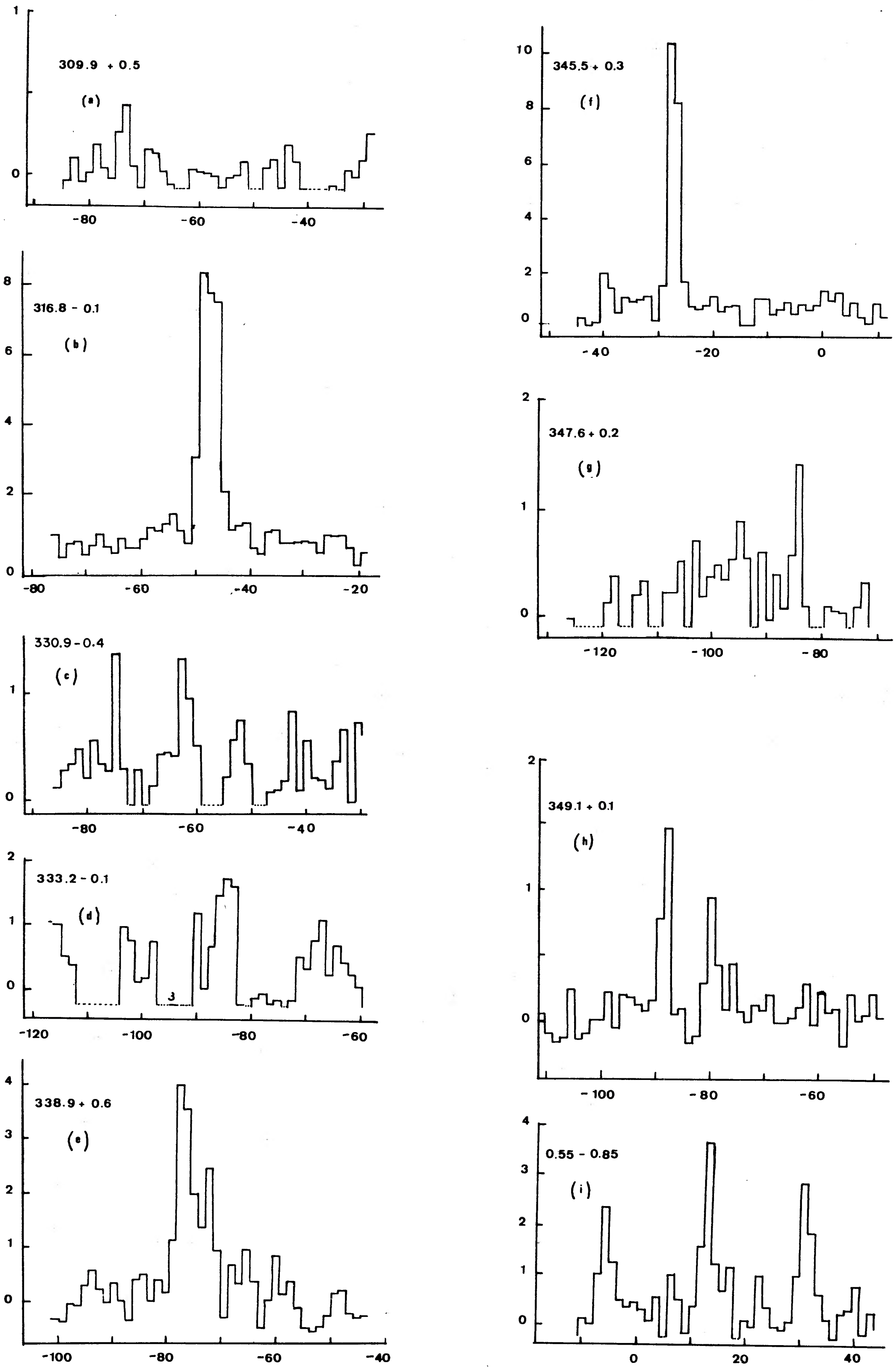

FIG. 2. Spectra of newly discovered H_2O sources associated with type-I OH emitters. All spectra are from Run I (November 1975) except for (a) and (h) (Run II: June 1976): (a) 309.9 + 0.5, (b) 316.8 − 0.1, (c) 330.9 − 0.4, (d) 333.2 − 0.1, (e) 338.9 + 0.6, (f) 345.5 + 0.3, (g) 347.6 + 0.2, (h) 349.1 + 0.1, (i) 0.55 − 0.85. Abcissae are in km sec^{-1} and ordinates in corrected antenna temperature (K).

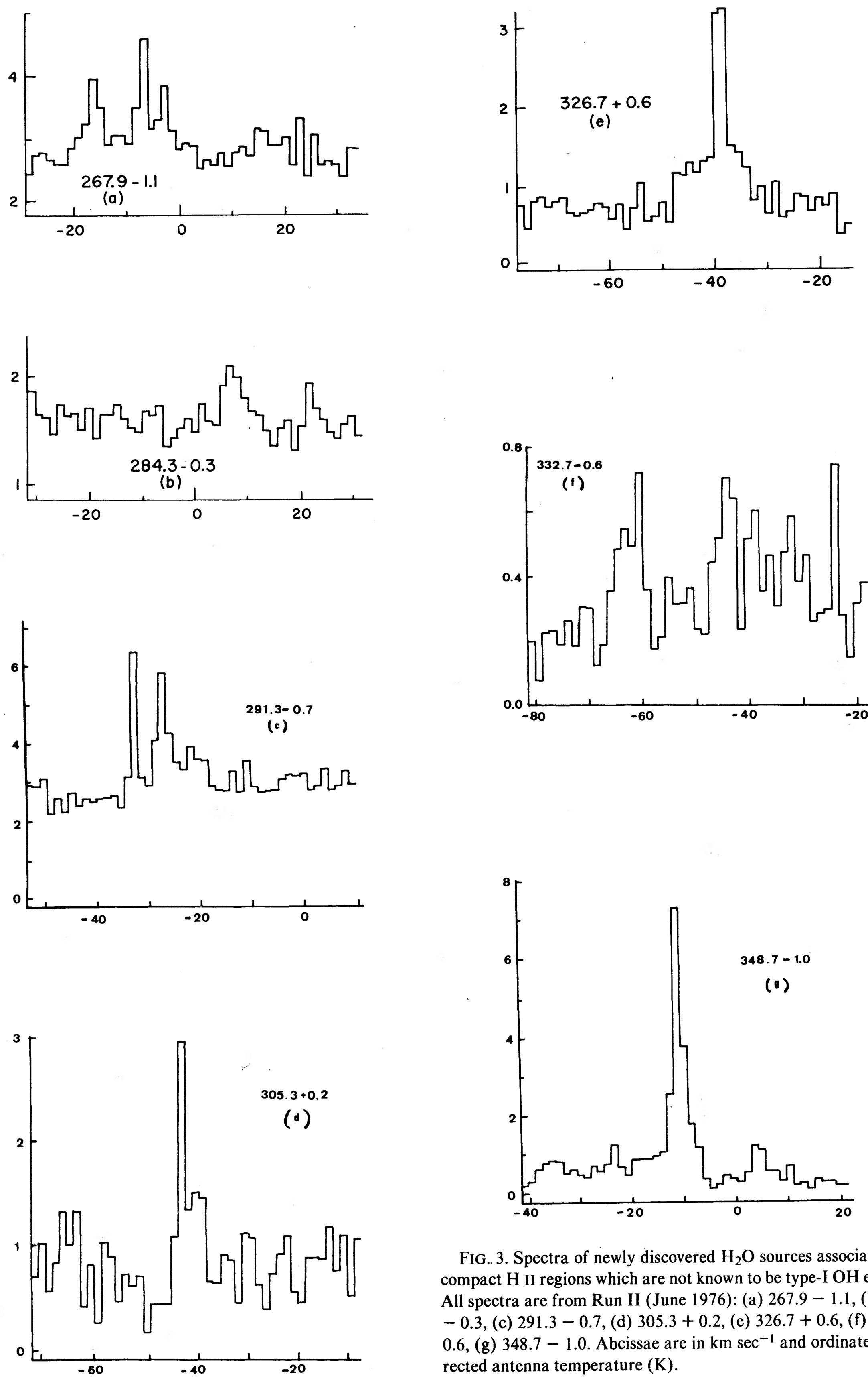

FIG. 3. Spectra of newly discovered H_2O sources associated with compact H II regions which are not known to be type-I OH emitters. All spectra are from Run II (June 1976): (a) 267.9 − 1.1, (b) 284.3 − 0.3, (c) 291.3 − 0.7, (d) 305.3 + 0.2, (e) 326.7 + 0.6, (f) 332.7 − 0.6, (g) 348.7 − 1.0. Abcissae are in km sec^{-1} and ordinates in corrected antenna temperature (K).

fact of a few faulty receiver channels. This source was discovered in Run I (Kaufmann *et al.* 1976), and was independently discovered by Knapp and Morris (1976).

B. Non-OH Sources

We examined all other compact H II regions with brightness temperature greater than 5 K as mapped in the 5-GHz continuum survey by Goss and Shaver (1970). Seven new H_2O celestial masers were found at H II regions for which no OH main-line emission had previously been known. These sources originally suggested the existence of another class of H_2O emitters (Kaufmann *et al.* 1976), with no associated type-I OH source, contrary to the predictions (Turner 1971; Turner and Rubin 1971). More recently, Haynes *et al.* (1976) found weak OH emission in the direction of three objects of this class, suggesting that the apparent lack of OH maser emission may really be a problem of flux detection limits.

The center radial velocity for each measurement was obtained from the H109α recombination line velocity (Wilson *et al.* 1970). The observed spectra are shown in Fig. 3, and the corresponding observational data in Table I(b). No attempt was made to determine actual H_2O source positions.

H_2O 267.9 − 1.1 [Fig. 3(a)]. Situated in the compact H II region RCW 38, with lines superimposed on a strong continuum. Three lines were found in Run II, at −3.4 km sec^{-1} (138 Jy), −7.4 km sec^{-1} (166 Jy), and −16.9 km sec^{-1} (143 Jy).

H_2O 284.3 − 0.3 [Fig. 3(b)]. Situated in RCW 49. Two lines found in Run II at 6.7 km sec^{-1} (75 Jy) and at 21.6 km sec^{-1} (70 Jy), superimposed on a 1.4-K continuum. During Run I only the 21.6-km sec^{-1} line (90 Jy) was found.

H_2O 291.3 − 0.7 [Fig. 3(c)]. Situated in the RCW 57 complex, at the position of a compact protostellar infrared object (Frogel and Persson 1974). Two lines at −27.4 km sec^{-1} (209 Jy) and −32.8 km sec^{-1} (229 Jy) were found in Run II. During Run I the −27.4-km sec^{-1} line was about one-half of the Run II measurements.

H_2O 305.3 + 0.2 [Fig. 3(d)]. Situated in the RCW 74 extended region. In Run I two lines were seen at −40 km sec^{-1} (53 Jy) and −42.7 km sec^{-1} (79 Jy). The figure shows the Run II result, when the measured fluxes were 55 and 107 Jy. We hesitate to report this as a new source, because of the possibility of confusion with H_2O 305.4 + 0.2 in which main lines were reported at −36.6 km sec^{-1} (85 Jy) and −31.9 km sec^{-1} (111 Jy) (Caswell *et al.* 1974).

H_2O 326.7 + 0.6 [Fig. 3(e)]. Possibly associated with RCW 95. Spectra were obtained centered at 52, 46, and −97.2 km sec^{-1} in the two runs to observe the complexity of the spectrum. Referring to Run II, lines are found at +24.1 km sec^{-1} (45 Jy), +6.9 km sec^{-1} (46 Jy), a broad line at −13.6 km sec^{-1} (54 Jy), and a strong line at −37.9 km sec^{-1} (116 Jy). The figure shows a Run II spectrum centered at −46 km sec^{-1}.

H_2O 332.7 − 0.6 [Fig. 3(f)]. Situated in the RCW 106 extended H II region. Several weak lines appear in the spectra obtained in the two runs. The figure is from Run II, where major lines appear at −23.0 km sec^{-1} (27 Jy), −44.6 km sec^{-1} (25 Jy), and at −60.8 km sec^{-1} (26 Jy), superimposed on a 0.25-K continuum.

H_2O 348.7 − 1.0 [Fig. 3(g)]. Situated in RCW 122. The figure shows the spectrum taken during Run II. A strong line (260 Jy) appears at −11.3 km sec^{-1}, and weaker features at −23.5 km sec^{-1} (43 Jy) and +3.5 km sec^{-1} (43 Jy). OH in absorption has been reported in this source at the velocity of the strong line (Turner 1970).

Another water vapor source was clearly seen in both runs at the position of 333.0 − 0.4 (65 Jy at −51.3 km sec^{-1} in Run I), but this could be confusion with H_2O 333.2 − 0.5 (Caswell *et al.* 1974). Finally, H_2O emission was observed in H2–3 during the 1973 survey (Kaufmann *et al.* 1974a), but not in the present survey, to an upper limit of 35 Jy. For this source Haynes *et al.* (1976) recently discovered a weak OH emission line at −18 km sec^{-1}.

C. Negative Results

In Tables II(a) and (b) we indicate the positions of both types of H II regions examined in the present survey from which no H_2O emission was found to the indicated upper flux limits. The results correspond to Run I, excepting, in Table II(a), 301.0 + 1.1, 308.9 + 0.1, and 340.1 − 0.2.

III. CARINA NEBULA

The Carina Nebula was observed at 18 compact bright points selected from continuum maps at 8.8 GHz (Hutchteier and Day 1975) and 22 GHz (Scalise Jr. *et al.* 1974). Central radial velocities were obtained from H109α recombination line studies (Gardner *et al.* 1970). No source of water vapor emission was found within the upper limits indicated in Table III where the 18-Jy limits were obtained in Run II, except possibly in 287.4 − 0.6, with an apparent 63-Jy line at −17.3 km sec^{-1}, superimposed on a 0.7-K continuum.

IV. MAGELLANIC CLOUDS

The Magellanic Clouds contain a large number of H II regions which are good candidates for H_2O maser emission. A strong source in the Large Magellanic Cloud similar to W49 would have a flux of about 1000 Jy and be easily detected at this distance. A normal source similar to Ori A would show lines of about 15 Jy and be only marginally detectable in the present survey.

We examined 23 points in the Large Magellanic Cloud that were probably thermal H II regions, with

TABLE II. Type-I OH sources and H II regions for which no H_2O emission was found.

Source	Observed positions (1950.0) R.A.	Dec.	Center of radial velocity searched (km sec^{-1})	Upper limits (Jy)
		(a) Type-I OH sources		
284.2 − 0.8	$10^h19^m42^s$	−57°50′06″	−5	50
301.0 + 1.1	12 32 00	−61 22 39	−40	18
308.9 + 0.1	13 39 37	−61 53 44	−50	14
320.2 − 0.3	15 06 00.3	−58 13 35	−70	30
324.2 + 0.1	15 29 01.8	−55 45 22	−90	45
328.2 − 0.5	15 54 04.9	−53 50 00	−70	60
329.0 − 0.2	15 56 44.8	−53 03 55	−38	70
329.2 − 0.3	15 57 55.3	−53 03 30	−53	60
329.4 − 0.5	15 59 41.1	−53 01 33	−70	40
331.4 − 0.3	16 08 35.8	−51 38 16	−70	40
337.7 − 0.1	16 34 49.8	−46 54 48	−50	60
338.9 − 0.1	16 39 29.4	−46 03 05	−40	40
339.6 − 0.1	16 42 30.1	−45 31 22	−36	45
340.1 − 0.2	16 44 39	−45 16 26	−40	14
353.4 − 0.3	17 26 53	−34 39 00	−20	50
355.4 + 0.1	17 30 18	−34 45 42	+20	50
		(b) H II regions without known OH emitters		
265.1 + 1.5	$08^h57^m39^s$	−43°33′36″	0	40
268.0 − 1.0	08 58 06	−47 20 12	+2	65
282.0 − 1.2	10 04 53	−56 57 30	+20	40
292.0 + 1.8	11 22 20	−58 59 24	−22	45
298.2 − 0.3	12 07 24	−62 33 18	+20	45
298.9 − 0.4	12 12 45	−62 44 48	+20	45
305.2 + 0.0	13 08 03	−62 29 12	−40	45
305.6 + 0.0	13 11 07	−62 28 54	−45	40
309.8 + 1.8	13 43 45	−60 07 18	−60	40
311.9 + 0.1	14 03 52	−61 13 06	−47	50
320.2 + 0.8	15 01 35	−57 19 24	−36	40
321.0 − 0.5	15 12 07	−58 00 30	−61	40
322.2 + 0.6	15 14 49	−56 27 54	−52	30
326.5 + 0.9	15 38 33	−53 48 54	−39	40
328.4 + 0.2	15 51 46	−53 08 36	−40	40
332.2 − 0.4	16 12 52	−51 10 06	−56	50
333.0 + 0.8	16 11 23	−49 42 18	−50	40
333.3 − 0.4	16 17 45	−50 19 18	−50	30
336.5 − 1.5	16 36 22	−48 46 18	−37	40
336.8 − 0.0	16 30 49	−47 30 24	−75	35
337.1 − 0.2	16 33 01	−47 25 18	−70	40
338.0 − 0.1A	16 36 27	−46 44 48	−80	45
338.0 − 0.1B	16 36 17	−46 46 48	−50, −75	35, 50
338.5 + 0.1	16 37 30	−46 13 54	−130	45
338.4 + 0.2	16 36 28	−46 16 06	−40	60
340.8 − 1.0	16 50 39	−45 12 12	−24	45
343.5 − 0.0	16 55 48	−42 30 12	−15, −30	40, 40
345.4 + 1.4	16 56 10	−40 07 00	−15	30
345.2 + 1.0	16 57 09	−40 29 18	−9	50
345.4 − 0.9	17 06 02	−41 31 47	0	40
351.0 + 0.7	17 16 26	−36 02 00	−4	50
351.2 + 0.5	17 17 33	−36 01 00	−3, −20	60, 60
353.2 + 0.9	17 21 30	−34 08 18	−3	75
353.1 + 0.6	17 22 18	−34 20 06	−3	65
353.1 + 0.7	17 22 22	−34 17 36	−3	100
351.6 + 1.3	17 25 53	−36 37 49	−10	70

completely negative results. The sources were selected from the 5-GHz continuum maps of McGee *et al.* (1972). Radial velocities were derived from H109α recombination line values, when available; from 21-cm maps; or from nominal "spiral arm" velocities (McGee and Milton 1966; McGee *et al.* 1974). In Table IV(a) we indicate the sources observed, the velocity range searched, and the corresponding upper flux limit. The reported values refer to Run I, with the exception of MC16 (+250 km sec^{-1}), MC18, MC33, MC69, MC74 (+255 km sec^{-1}), and MC77.

In the Small Magellanic Cloud, four H II regions (Henize 1956) were examined for H_2O emission, also with negative results. They are listed in Table IV(b).

V. SUMMARY

We report the completion of the first two experimental runs (8 days total) with the newly installed *K*-band maser. A wide-ranging survey has been carried out of a number of classes of H_2O emitters, with gratifying results. Using a system with upper detection limits 2–3 times better than previous searches, the number of known H_2O masers associated with H II regions in the

TABLE III. Positions in Carina Nebula searched for H_2O emission.

Source	Positions observed (1950.0) R.A.	Dec.	Center of radial velocity searched (km sec^{-1})	Upper limit for detection (Jy)	Comments
284.7 + 0.3	10^{h}27^{m}36^s	−57°10′12″	−20	40	
286.2 − 0.1	10 35 16	−58 18 54	−20	70	
287.2 − 0.8	10 40 30	−59 24 00	−20	18	Car IV compact H II region (Scalise Jr. *et al.* 1974).
287.4 − 0.6	10 41 39	−59 19 00	−20	18	Possible H_2O source Car I compact H II source (Gardner *et al.* 1970).
287.5 − 0.7	10 42 00	−59 24 00	−20	18	Car III compact H II region (Scalise Jr. *et al.* 1974).
	10 42 30	−59 08 00	−20	75	
287.6 − 0.6	10 42 54	−59 22 00	−20	18	Car II compact H II region (Gardner *et al.* 1970).
287.2 − 0.0	10 42 55	−58 38 24	−20	25	
	10 43 00	−59 20 00	−20	65	
	10 43 00	−59 24 00	−20	40	
η Car	10 43 15	−59 25 06	−20	25	Star
287.8 − 0.8	10 43 46	−59 39 00	−20	20	
287.9 − 1.0	10 43 49	−59 52 00	−20	40	
287.7 − 0.6	10 44 06	−59 30 00	−20	35	
289.1 − 0.3	10 54 28	−59 48 54	−20	55	
289.7 − 1.1	10 56 42	−60 49 54	−20	30	
289.9 − 0.8	10 59 00	−60 33 48	−20	55	
290.2 − 0.7	11 01 23	−60 38 48	−20	45	

TABLE IV. H II regions searched for H_2O emissions in the Magellanic Clouds.

Source	Observed position (1950.0) R.A.	Dec.	Center of radial velocity searched (km sec^{-1})	Upper limit for detection (Jy)
		(a) Large Magellanic Cloud		
MC 12	04^{h}51^{m}58^s	−66°59′48″	+310	25
MC 13	04 52 10	−69 27 00	+230	35
MC 16	04 54 35	−69 15.48	+250, +300	7, 40
MC 18	04 56 44	−66 28 24	+280	11
MC 19	04 57 33	−68 29 30	+250	45
MC 23	05 10 04	−68 56 24	+250	35
MC 24	05 13 37	−69 25 30	+250	35
MC 30	05 19 07	−69 16 24	+250	30
MC 33	05 23 11	−68 04 54	+310	18
MC 46	05 26 33	−67 30 48	+310	30
MC 50	05 27 56	−67 28 18	+280	35
MC 54	05 32 04	−71 05 48	+230	35
MC 58	05 32 30	−66 28 48	+280	25
MC 64	05 35 31	−67 36 00	+280	30
MC 69	05 36 08	−69 14 12	+255	11
MC 71	05 36 18	−69 40 18	+250	20
MC 74	05 39 04	−69 06 30	+230, +280, +255, +330	30, 20, 11, 25
MC 75	05 39 37	−69 30 54	+250	25
MC 77	05 40 24	−69 46 00	+280	7
MC 78	05 40 40	−69 21 30	+230	25
MC 79	05 42 32	−69 67 54	+250	25
MC 80	05 42 34	−71 20 42	+230	30
MC 82	05 43 02	−69 05 30	+150	30
MC 91	05 49 27	−70 05 00	+230	20
		(b) Small Magellanic Cloud		
SMC 66	00^{h}57^{m}30^s	−72°27′00″	+150	15
SMC 78	01 03 30	−72 15 00	+150	15
SMC 83	01 12 30	−73 33 00	+150	20
SMC 84	01 12 18	−73 35 00	+150	25

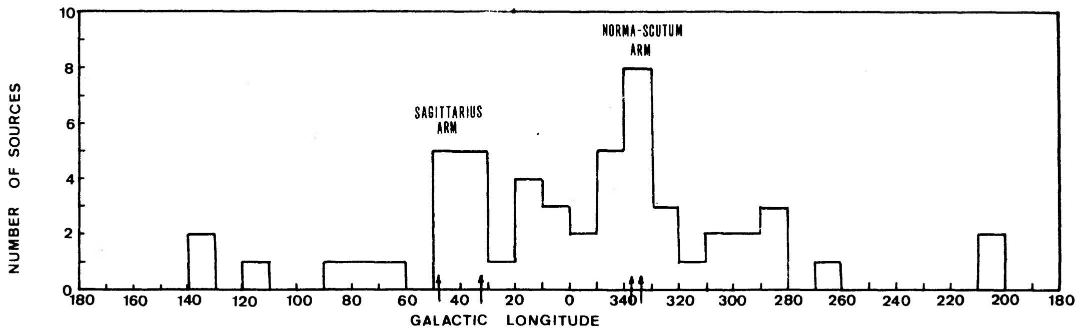

FIG. 4. Distribution of all known galactic nonstellar H_2O (maser) sources as a function of Galactic longitude. Arrows indicate concentrations of H II regions, along the spiral arms as named.

southern hemisphere has been nearly doubled. H_2O emitters found not to be collocated with known type-I OH sources suggest the presence of new low-flux-level OH sources, possibly associated with regions of star formation as found in a recent high-sensitivity survey in the northern hemisphere (Lo *et al.* 1975).

The total number of known Galactic H_2O sources in both hemispheres is now 53, including the 16 reported here and excluding stars and IR objects. Figure 4 is a histogram of the distribution of these sources with Galactic longitude, an extension of the plot by Johnston *et al.* (1972). Not surprisingly, there is an evident concentration of H_2O sources toward the central region of the Galaxy, with peaks roughly coinciding with tangents to known spiral arms.

We consider that the present experiment should be repeated with improved atmospheric conditions at Itapetinga. Values of τ will then range typically between 0.10 and 0.25 and there will be fewer interruptions due to clouds and rain. This factor, added to minor technical improvements still required by the system, may permit an improvement of 2–3 times in upper detection limit.

We wish to express our gratitude for the technical assistance rendered by J. C. Raffaelli, E. H. Koppe, A. L. Ibañez, P. Marques dos Santos, V. Saraceni, R. Hadano, A. M. G. Balboa, and M. Shimabukuro at Itapetinga, and by J. C. Carter, J. Sobolewski, N. Lariviere, and R. Erickson at Haystack. We also are grateful to the Department of Physics of Campinas State University, Campinas, São Paulo, Brasil, and Professor D. Pinatti for their indispensable assistance in liquefying the helium needed for the operation of the *K*-band maser.

This joint research project is a result of a bilateral scientific agreement established between the U.S. and Brazilian governments. Support was received from the Brazilian research agency Conselho Nacional de Desenvolvimento Científico e Technológico (CNPq Proc. No. 13.364/72-C), and from the U.S. research agency, the National Science Foundation (NSF), under Grant No. 01P73-07417A02. Haystack Observatory is operated by the Massachusetts Institute of Technology for the Northeast Radio Observatory Corporation (NEROC), under NSF Grant AST 75-14701.

REFERENCES

Caswell, J. L., Batchelor, R. A., Haynes, R. F., and Huchtmeier, W. K. (1974), Aust. J. Phys. **27**, 417.

Caswell, J. L., and Haynes, R. F. (1975), Aust. J. Phys. To be published.

Fogarty, W. G. (1975). IEEE Trans. Antennas Propag. **AP23**, 441.

Frogel, J. A., and Persson, S. E. (1974). Astrophys. J. **192**, 351.

Gardner, F. F., Milne, O. K., Mezger, P. G., and Wilson, T. L. (1970). Astron. Astrophys. **7**, 349.

Gardner, F. F., and Whiteoak, J. B. (1975). Aust. J. Phys. To be published.

Goss, W. M., and Shaver, P. A. (1970). Aust. J. Phys. Astrophys. Suppl. No. 14.

Goss, W. M., Knowles, S. H., Balister, M., Batchelor, R. A., and Wellington, K. J. (1975). Aust. J. Phys. To be published.

Haynes, R. F., Caswell, J. L., and Goss, W. M. (1976). Aust. J. Phys. To be published.

Huchtmeier, W. K., and Day, G. A. (1975). Astron. Astrophys. **153**, 164.

Johnston, K. J., Knowles, S. H., and Sullivan, W. T III (1971). Astrophys. J. Lett. **167**, L93.

Johnston, K. J., Robinson, B. J., Caswell, J. L., and Batchelor, R. A. (1972). Astrophys. Lett. **10**, 93.

Kauffman, P., Fogarty, W. G., Scalise, E., Jr., and Schaal, R. E. (1974a). Astron. J. **79**, 933.

Kaufmann, P., Fogarty, W. G., Scalise, E., Jr., and Schaal, R. E. (1974b). In *Galactic Radio Astronomy,* edited by F. J. Kerr and S. C. Simenson III (Reidel, Dordrecht), p. 293.

Kaufmann, P., Fogarty, W. G., Koppe, E. H., Marques dos Santos, P., Scalise, E., Jr., Schaal, R. E., and Tiba, T. (1976). Rev. Bras. Tecnol. **7**, 81.

Kaufmann, P., Gammon, R. H., Ibañez, A. L., Lépine, J. R. D., Marques dos Santos, P., Paes de Barros, M. H., Scalise, E., Jr., Schaal, R. E., Zisk, S., Carter, J. C., Meeks, M. L., and Sobolowsky, J. M. (1976). Nature **260**, 306.

Klein, M. J. (1974). Astron. J. **79**, 139.

Knapp, G. R., and Morris, M. (1976). Astrophys. J. To be published.

Kukarkin, B. V., Kholopov, P. N., Efremov, Yu, N., Kukarkin, N. P.,

Kurichkin, N. E., Medvedeva, G. I., Perova, N. B., Fedorovich, V. P., and Frolov, M. S. (1969). *General Catalogue of Variables Stars* (Sternb. State Astron. Inst., Moscow), 3rd ed.
Law, S. E., and Staelin, D. H. (1968). Astrophys. J. **154,** 1077.
Lépine, J. R. D. (1977). Ph.D. thesis, Univ. Paris.
Lo, K. Y., Burke, B. F., and Haschick, A. D. (1975). Astrophys. J. **207,** 81.
Marques dos Santos, P., Lazzareschi, J. R., and Golizia, J. M. (1974). Rev. Bras. Tecnol. **5,** 61.
Mc Gee, R. X., and Milton, J. A. (1966). Aust. J. Phys. **19,** 343.
Mc Gee, R. X., Brooks, J. W., and Batchelor, R. A. (1972). Aust. J. Phys. **25,** 581.
Mc Gee, R. X., Newton, L. M., and Brooks, J. W. (1974). Aust. J. Phys. **22,** 729.
Robinson, B. J., Caswell, J. L., and Goss, W. M. (1974). Aust. J. Phys. **27,** 575.
Scalise, E., Jr., Kaufmann, P., and Alcina, B. M. (1974). Nature **252,** 663.
Schwartz, P. R., Harvey, P. M., and Barrett, A. H. (1974). Astrophys. J. **187,** 491.
Turner, B. E. (1971). In *Highlights of Astronomy,* edited by C. de Jager (Reidel, Dordrecht), p. 378.
Turner, B. E., and Rubin, R. H. (1971). Astrophys. J. Lett. **170,** L113.
Wilson, T. L., Mezger, P. G., Gardner, F. F., and Milne, D. K. (1970). Astron. Astrophys. **6,** 364.
Yngvesson, K. S., Cardiasmenos, A. G., Shanley, J. F., Rydbeck, O. E. H., and Elldér, J. (1975). Astrophys. J. **195,** 91.